We are IntechOpen,
the world's leading publisher of
Open Access books
Built by scientists, for scientists

6,900
Open access books available

185,000
International authors and editors

200M
Downloads

154
Countries delivered to

Our authors are among the

TOP 1%
most cited scientists

12.2%
Contributors from top 500 universities

CLARIVATE ANALYTICS
BOOK CITATION INDEX
INDEXED

WEB OF SCIENCE™

Selection of our books indexed in the Book Citation Index
in Web of Science™ Core Collection (BKCI)

Interested in publishing with us?
Contact book.department@intechopen.com

Adaptive Sliding Mode Control of Adhesion Force in Railway Rolling Stocks

Jong Shik Kim, Sung Hwan Park,
Jeong Ju Choi and Hiro-o Yamazaki
School of Mechanical Engineering, Pusan National University
Republic of Korea

1. Introduction

Studies of braking mechanisms of railway rolling stocks focus on the adhesion force, which is the tractive friction force that occurs between the rail and the wheel (Kadowaki, 2004). During braking, the wheel always slips on the rail. The adhesion force increases or decreases according to the slip ratio, which is the difference between the velocity of the rolling stocks and the tangential velocity of each wheel of the rolling stocks normalized with respect to the velocity of the rolling stocks. A nonzero slip ratio always occurs when the brake caliper holds the brake disk, and thus the tangential velocity of the wheel so that the velocity of the wheel is lower than the velocity of the rolling stocks. Unless an automobile is skidding, the slip ratio for an automobile is always zero. In addition, the adhesion force decreases as the rail conditions change from dry to wet (Isaev, 1989). Furthermore, since it is impossible to directly measure the adhesion force, the characteristics of the adhesion force must be inferred based on experiments (Shirai, 1977).

To maximize the adhesion force, it is essential to operate at the slip ratio at which the adhesion force is maximized. In addition, the slip ratio must not exceed a specified value determined to prevent too much wheel slip. Therefore, it is necessary to characterize the adhesion force through precise modeling.

To estimate the adhesion force, observer techniques are applied (Ohishi, 1998). In addition, based on the estimated value, wheel-slip brake control systems are designed (Watanabe, 2001). However, these control systems do not consider uncertainty such as randomness in the adhesion force between the rail and the wheel. To address this problem, a reference slip ratio generation algorithm is developed by using a disturbance observer to determine the desired slip ratio for maximum adhesion force. Since uncertainty in the traveling resistance and the mass of the rolling stocks is not considered, the reference slip ratio, at which adhesion force is maximized, cannot always guarantee the desired wheel slip for good braking performance.

In this paper, two models are developed for the adhesion force in railway rolling stocks. The first model is a static model based on a beam model, which is typically used to model automobile tires. The second model is a dynamic model based on a bristle model, in which the friction interface between the rail and the wheel is modeled as contact between bristles (Canudas de Wit, 1995). The validity of the beam model and bristle model is verified through an adhesion test using a brake performance test rig.

We also develop wheel-slip brake control systems based on each friction model. One control system is a conventional PI control scheme, while the other is an adaptive sliding mode control (ASMC) scheme. The controller design process considers system uncertainties such as the traveling resistance, disturbance torque, and variation of the adhesion force according to the slip ratio and rail conditions. The mass of the rolling stocks is also considered as an uncertain parameter, and the adaptive law is based on Lyapunov stability theory. The performance and robustness of the PI and adaptive sliding mode wheel-slip brake control systems are evaluated through computer simulation.

2. Wheel-slip mechanism for rolling stocks

To reduce braking distance, automobiles are fitted with an anti-lock braking system (ABS) (Johansen, 2003). However, there is a relatively low adhesion force between the rail and the wheel in railway rolling stocks compared with automobiles. A wheel-slip control system, which is similar to the ABS for automobiles, is currently used in the brake system for railway rolling stocks.

The braking mechanism of the rolling stocks can be modeled by

$$F_a = \mu(\lambda)N \tag{1}$$

$$\lambda = \frac{v - r\omega}{v} \tag{2}$$

where F_a is the adhesion force, $\mu(\lambda)$ is the dimensionless adhesion coefficient, λ is the slip ratio, N is the normal force, v is the velocity of the rolling stocks, and ω and r are the angular velocity and radius of each wheel of the rolling stocks, respectively. The velocity of the rolling stocks can be measured (Basset, 1997) or estimated (Alvarez, 2005). The adhesion force F_a is the friction force that is orthogonal to the normal force. This force disturbs the motion of the rolling stocks desirably or undesirably according to the relative velocity between the rail and the wheel. The adhesion force F_a changes according to the variation of the adhesion coefficient $\mu(\lambda)$, which depends on the slip ratio λ, railway condition, axle load, and initial braking velocity, that is, the velocity at which the brake is applied. Figure 1 shows a typical shape of the adhesion coefficient $\mu(\lambda)$ according to the slip ratio λ and rail conditions.

To design a wheel-slip control system, it is useful to simplify the dynamics of the rolling stocks as a quarter model based on the assumption that the rolling stocks travel in the longitudinal direction without lateral motion, as shown in Fig. 2 the equations of motion for the quarter model of the rolling stocks can be expressed as

$$J\dot{\omega} = -B\omega + T_a - T_b - T_d \tag{3}$$

$$M\dot{v} = -F_a - F_r \tag{4}$$

where B is the viscous friction torque coefficient between the brake pad and the wheel, $T_a = rF_a$ and T_b are the adhesion and brake torques, respectively, T_d is the disturbance torque due to the vibration of the brake caliper, J and r are the inertia and radius, respectively, of each wheel of the rolling stocks, and M and F_r are the mass and traveling resistance force of the rolling stocks, respectively.
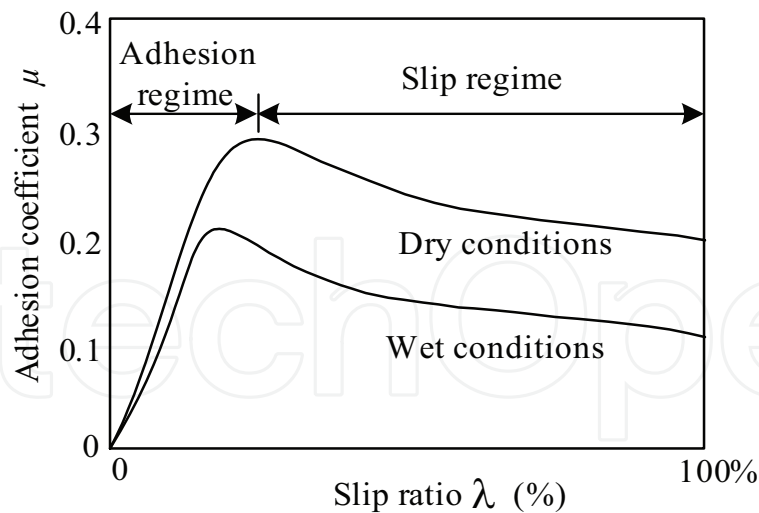
Fig. 1. Typical shape of the adhesion coefficient according to the slip ratio and rail conditions.
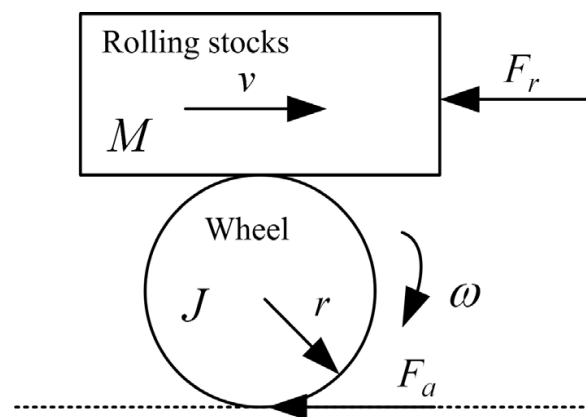

Fig. 2. Quarter model of the rolling stocks.

From (3) and (4), it can be seen that, in order to achieve sufficient adhesion force, a large brake torque T_b must be applied. When T_b is increased, however, the slip ratio increases, which causes the wheel to slip. When the wheel slips, it may develop a flat spot on the rolling surface. This flat spot affects the stability of the rolling stocks, the comfort of the passengers, and the life cycle of the rail and the wheel. To prevent this undesirable braking situation, a desired wheel-slip control is essential for the brake system of the rolling stocks.

In addition, the adhesion force between the wheel and the contact surface is dominated by the initial braking velocity, as well as by the mass M and railway conditions. In the case of automobiles, which have rubber pneumatic tires, the maximum adhesion coefficient changes from 0.4 to 1 according to the road conditions and the materials of the contact surface (Yi, 2002). In the case of railway rolling stocks, where the contact between the wheel and the rail is that of steel on steel, the maximum adhesion force coefficient changes from approximately 0.1 to 0.4 according to the railway conditions and the materials of the contact surface (Kumar, 1996). Therefore, railway rolling stocks and automobiles have significantly different adhesion force coefficients because of different materials for the rolling and contact surfaces. However, the brake characteristics of railway rolling stocks (Jin, 2004) and automobiles (Li, 2006) are similar.

According to adhesion theory, the maximum adhesion force occurs when the slip ratio is approximately between 0.1 and 0.4 in railway rolling stocks. Therefore, the slip ratio at which the maximum adhesion force is obtained is usually used as the reference slip ratio for the brake control system of the rolling stocks. Figure 3 shows an example of a wheel-slip control mechanism based on the relationship between the slip ratio and braking performance.
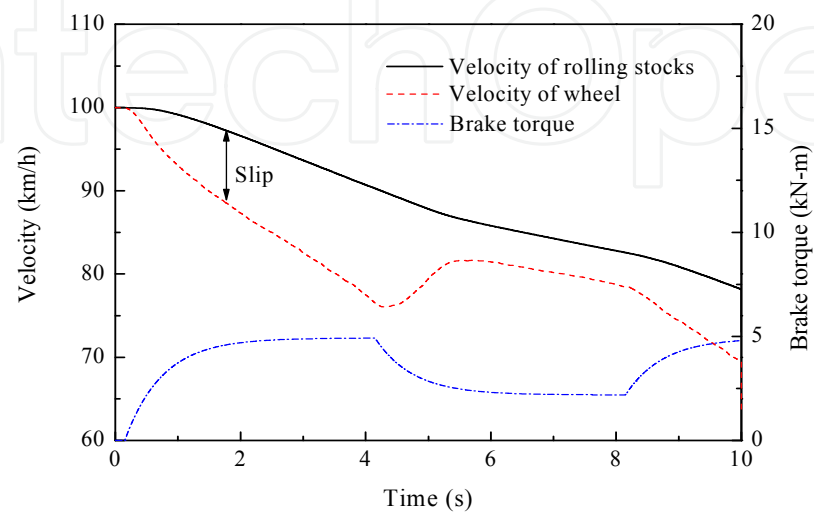

Fig. 3. Example of a wheel-slip control mechanism based on the relationship between the slip ratio and braking performance.
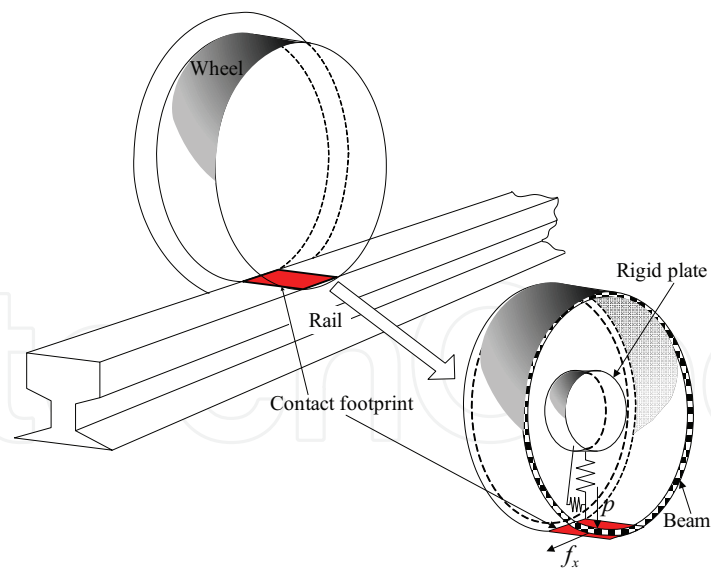

Fig. 4. Simplified contact model for the rail and wheel.

3. Static adhesion force model based on the beam model

To model the adhesion force as a function of the slip ratio, we consider the beam model, which reflects only the longitudinal adhesion force. Figure 4 shows a simplified contact model for the rail and wheel, where the beam model treats the wheel as a circular beam

supported by springs. The contact footprint of an automobile tire is generally approximated as a rectangle by the beam model (Sakai, 1987). In a similar manner, the contact footprint between the rail and the wheel is approximated by a rectangle as shown in Fig. 5.
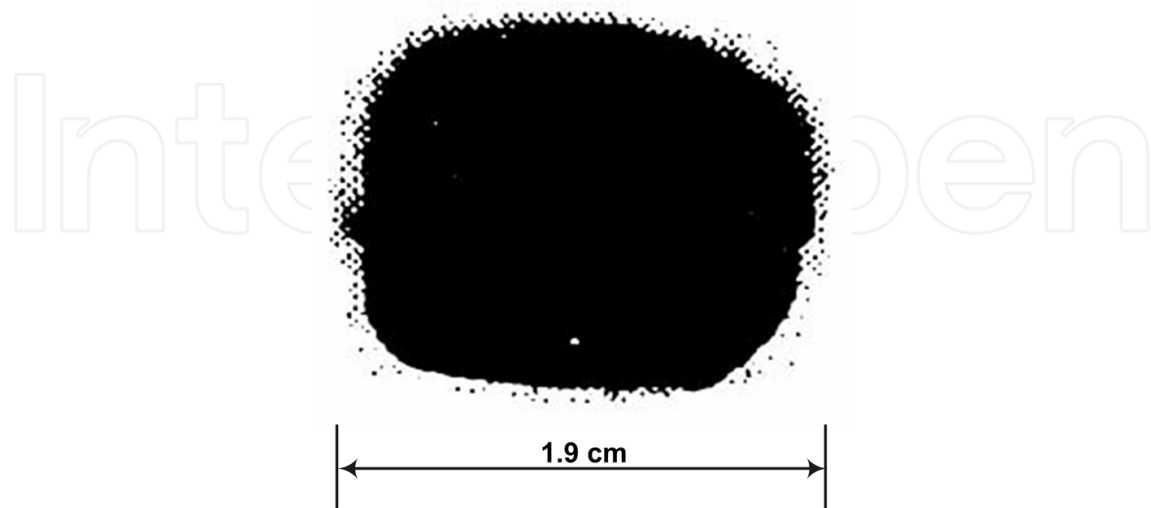

Fig. 5. Contact footprint between the rail and the wheel.

The contact pressure p between the rail and the wheel at the displacement x_c from the tip of the contact footprint in the longitudinal direction is given by (Sakai, 1987)

$$p = \frac{6N}{l^3 w}\left[\left(\frac{l}{2}\right)^2 - \left(x_c - \frac{l}{2}\right)^2\right]$$

(5)

where N is the normal force, and l and w are the length and width of the contact footprint, respectively. Figure 6 shows a typical distribution of the tangential force coefficient in a contact footprint (Kalker, 1989).

In Fig. 6, the variable f_x, which is the derivative of the adhesion force F_a with respect to the displacement x_c from the tip of the contact footprint, is given by

$$f_x = \begin{cases} C_x \lambda w x_c & \text{for } 0 \le x_c \le l_h, \\ \mu_d p & \text{for } l_h < x_c \le l, \end{cases}$$

(6)

where C_x is the modulus of transverse elasticity, l_h is the displacement from the tip of the contact footprint at which the adhesion-force derivative f_x changes rapidly, and μ_d is the dynamic friction coefficient. In particular, μ_d is defined by

$$\mu_d = \mu_{\max} - \frac{a\lambda v l}{(l - l_h)}$$

(7)

where $\mu_{\max}$ is the maximum adhesion coefficient, a is a constant that determines the dynamic friction coefficient in the slipping regime, and l_h is expressed as (Sakai, 1987)

$$l_h = l\left(1 - \frac{K_x \lambda}{3\mu_{\max} N}\right)$$

(8)

where K_x is the traveling stiffness calculated by

$$K_x = \frac{1}{2} C_x l^2 \tag{9}$$

The wheel load, which is the normal force, is equal to the integrated value of the contact pressure between the rail and the wheel over the contact footprint. Therefore, the adhesion force F_a between the rail and the wheel can be calculated by integrating (6) over the length of the contact footprint and substituting (7) and (8) into (6), which is expressed as

$$F_a = \frac{1}{2} C_x \lambda w l^2 \left(1 - \frac{K_x \lambda}{3\mu_{\max}N}\right)^2 + \frac{1}{2} K_x \lambda - \frac{3}{2} Na(v - r\omega)$$
$$- \frac{1}{2}\mu_{\max}N\left[1 - 3\frac{Na(v - r\omega)}{K_x\lambda}\right]\left[1 - \left(1 - \frac{2K_x\lambda}{3\mu_{\max}N}\right)^3\right]. \tag{10}$$
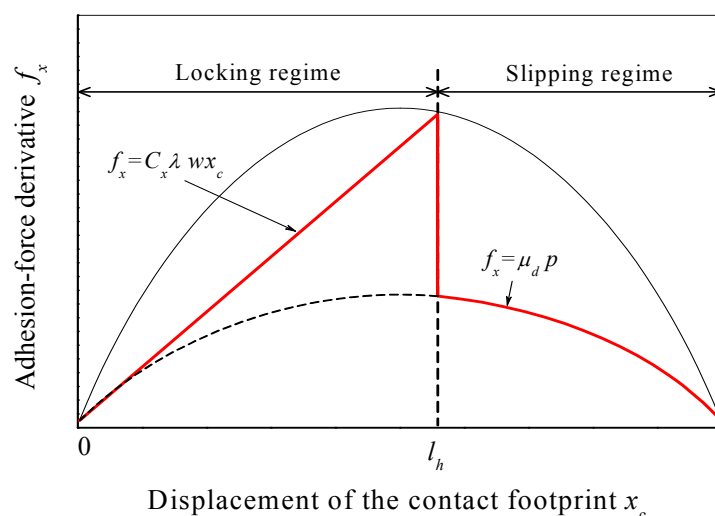

Fig. 6. A typical distribution of the tangential force coefficient in a contact footprint.

4. Dynamic adhesion force model based on bristle contact

As a dynamic adhesion force model, we consider the Dahl model given by (Dahl, 1976)

$$\frac{dz}{dt} = \sigma - \frac{\alpha|\sigma|}{F_c}z \tag{11}$$

$$F = \alpha z \tag{12}$$

where z is the internal friction state, σ is the relative velocity, α is the stiffness coefficient, and F and F_c are the friction force and Coulomb friction force, respectively. Since the steady-state version of the Dahl model is equivalent to Coulomb friction, the Dahl model is a generalized model for Coulomb friction. However, the Dahl model does not capture either the Stribeck effect or stick-slip effects. In fact, the friction behavior of the adhesion force

according to the relative velocity σ for railway rolling stocks exhibits the Stribeck effect, as shown in Fig. 7. Therefore the Dahl model is not suitable as an adhesion force model for railway rolling stocks.
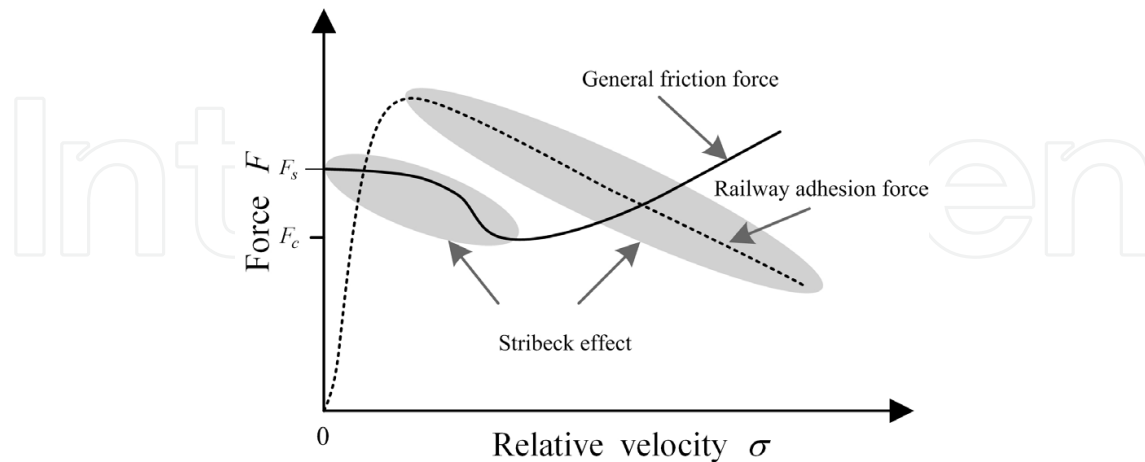

Fig. 7. Typical shape of the general friction force and adhesion force in railway rolling stocks according to the relative velocity.

However, the LuGre model (Canudas de Wit, 1995), which is a generalized form of the Dahl model, can describe both the Stribeck effect and stick-slip effects. The LuGre model equations are given by

$$\frac{dz}{dt} = \sigma - \frac{\alpha |\sigma|}{g(\sigma)} z \tag{13}$$

$$g(\sigma) = F_c + (F_s - F_c) e^{-(\sigma/v_s)^2} \tag{14}$$

$$F = \alpha z + \alpha_1 \dot{z} + \alpha_2 \sigma \tag{15}$$

where z is the average bristle deflection, v_s is the Stribeck velocity, and F_s is the static friction force. In addition, α, α_1, and α_2 are the bristle stiffness coefficient, bristle damping coefficient, and viscous damping coefficient, respectively.

The functions $g(\sigma)$ and F in (14) and (15) are determined by selecting the exponential term in (14) and coefficients α, α_1, and α_2 in (15), respectively, to match the mathematical model with the measured friction. For example, to match the mathematical model with the measured friction, the standard LuGre model is modified by using $e^{-|\sigma/v_s|^{\frac{1}{2}}}$ in place of the term $e^{-(\sigma/v_s)^2}$ in (14). Furthermore, for the tire model for vehicle traction control, the function F given by (15) is modified by including the normal force. Thus, (13)-(15) are modified as (Canudas de Wit, 1999)

$$\frac{dz}{dt} = \sigma - \frac{\alpha' |\sigma|}{g(\sigma)} z \tag{16}$$

$$g(\sigma) = \mu_c + (\mu_s - \mu_c) e^{-|\sigma/v_s|^{\frac{1}{2}}} \tag{17}$$

$$F = (\alpha' z + \alpha_1' \dot{z} + \alpha_2' \sigma)N \tag{18}$$

where μ_s and μ_c are the static friction coefficient and Coulomb friction coefficient, respectively, $N = mg$ is the normal force, m is the mass of the wheel, and $\alpha' = \dfrac{\alpha}{N}$, $\alpha_1' = \dfrac{\alpha_1}{N}$, and $\alpha_2' = \dfrac{\alpha_2}{N}$ are the normalized wheel longitudinal lumped stiffness coefficient, normalized wheel longitudinal lumped damping coefficient, and normalized viscous damping coefficient, respectively.

In general, it is difficult to measure and identify all six parameters, α, α_1, α_2, F_s, F_c, and v_s in the LuGre model equations. In particular, identifying friction coefficients such as α and α_1 requires a substantial amount of experimental data (Canudas de Wit, 1997). We thus develop a dynamic model for friction phenomena in railway rolling stocks, as shown in Fig. 7. The dynamic model retains the simplicity of the Dahl model while capturing the Stribeck effect.

As shown in Fig. 8 (Canudas de Wit, 1995), the motion of the bristles is assumed to be the stress-strain behavior in solid mechanics, which is expressed as

$$\frac{dF_a}{dx} = \alpha\left[1 - h(\sigma)F_a\right] \tag{19}$$

where F_a is the adhesion force, α is the coefficient of the dynamic adhesion force, and x and σ are the relative displacement and velocity of the contact surface, respectively. In addition, the function $h(\sigma)$ is selected according to the friction characteristics.
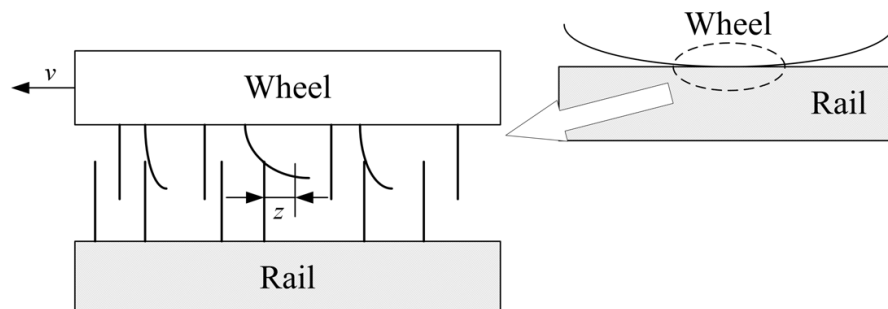

Fig. 8. Bristle model between the rail and the wheel.

Defining z to be the average deflection of the bristles, the adhesion force F_a is assumed to be given by

$$F_a = \alpha z \tag{20}$$

The derivative of F_a can then be expressed as

$$\frac{dF_a}{dt} = \frac{dF_a}{dx}\frac{dx}{dt} = \frac{dF_a}{dx}\sigma = \alpha\left[1 - h(\sigma)F_a\right]\sigma = \alpha\frac{dz}{dt} \tag{21}$$

It follows from (20) and (21) that the internal state z is given by

$$\dot{z} = \sigma\left[1 - h(\sigma)F_a\right] = \sigma\left[1 - \alpha h(\sigma)z\right]. \tag{22}$$

To select the function $h(\sigma)$ for railway rolling stocks, the term $e^{-\sigma/v_s}$ is used in place of $e^{-(\sigma/v_s)^2}$ in (14). This term is simplified by executing the Taylor series expansion for $e^{-\sigma/v_s}$ and by taking only the linear term $1 - \dfrac{\sigma}{v_s}$. In addition, neglecting the coefficients α_1 and α_2 in (15) for simplicity yields

$$g(\sigma) = F_c + (F_s - F_c)\left(1 - \frac{\sigma}{v_s}\right) = F_s - (F_s - F_c)\frac{\sigma}{v_s}. \tag{23}$$

By comparing (13) and (23) with (22) and by considering the relative velocity σ, which is positive in railway rolling stocks, $h(\sigma)$ in (22) can be derived as

$$h(\sigma) = \frac{\beta}{\gamma - \sigma} \tag{24}$$

where $\beta = \dfrac{1}{F_s - F_c}v_s$ and $\gamma = \dfrac{F_s}{F_s - F_c}v_s$. In general, β and γ are positive tuning parameters because F_s is larger than F_c as shown in Fig. 7 In the dynamic model, the parameter α is the coefficient for the starting point of the slip regime, where the adhesion force decreases according to the relative velocity, and the parameters β and γ are the coefficients for the slope and shift in the slip regime, respectively.

5. Verification of the adhesion force models

To verify the adhesion force models, experiments using a braking performance test rig in the Railway Technical Research Institute in Japan and computer simulations are carried out under various initial braking velocity conditions. Figure 9 shows the test rig for the braking performance test. The conceptual schematic diagram is shown in Fig. 10. This test rig consists of a main principal axle with a wheel for rolling stocks on a rail, flywheels, a main motor, a sub-axle with a wheel, and a brake disk. After accelerating to the target velocity by the main motor, the brake caliper applies a brake force to the wheel. The inertia of the flywheels plays the role of the inertia of the running railway rolling stocks.
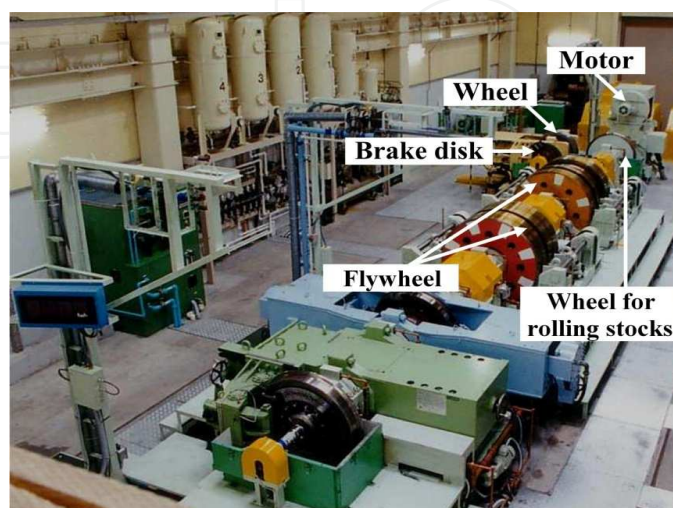
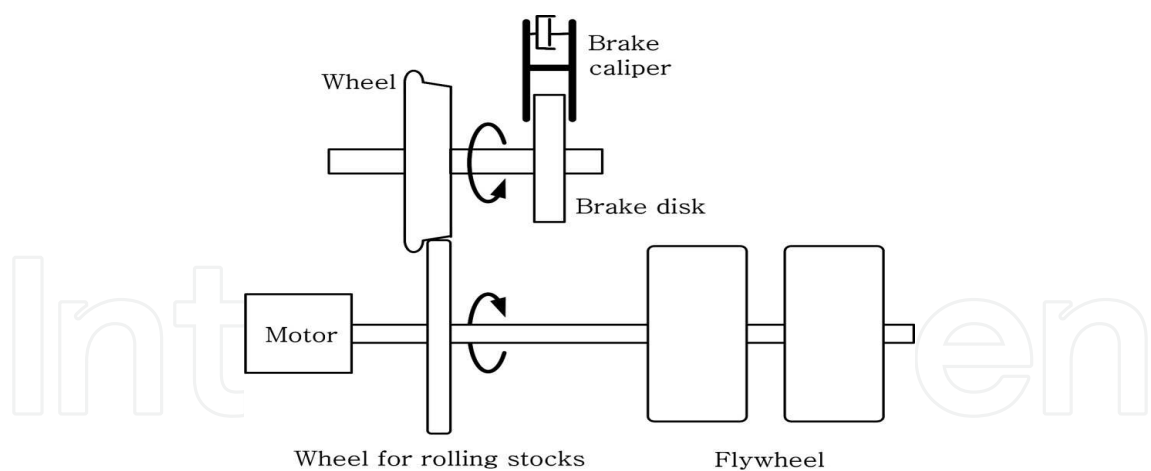

Fig. 9. Test rig for the brake performance test.

Fig. 10. Conceptual schematic diagram of the test rig for the brake performance test.

The test conditions are shown in Table 1. During the experiments, the brake torque T_b, the wheel load N, the angular velocity of the wheel ω, and the velocity of the rolling stocks v are measured simultaneously. The adhesion torque T_a between the rail and the wheel used in the calculation of the adhesion coefficient is also estimated in real time. As in the case of running vehicles, it is impossible to measure the adhesion torque directly on the brake performance test rig.

Test Condition	Value
Initial braking velocity	30, 60, 100, 140 km/h
Slip ratio	0 – 50%
Wheel load	34.5 kN
Wheel inertia	60.35 kg-m²
Viscous friction torque coefficient	0.25 N-m-s

Table 1. Test conditions of the test rig for the brake performance test

It is essential that knowledge of the adhesion torque be available for both ABS in automobiles and wheel-slip control of rolling stocks. However, it is difficult to directly acquire this information. While an optical sensor, which is expensive (Basset, 1997), can be used to acquire this information, the adhesion force between the wheel and the rail is estimated through the application of a Kalman filter (Charles, 2006). By using this scheme, the adhesion force can be estimated online during the normal running of the vehicle before the brake is applied. A disturbance observer considering the first resonant frequency of the rolling stocks is designed in order to avoid undesirably large wheel slip, which causes damage to the rail and wheel (Shimizu, 2007). A sliding mode adhesion-force observer using the estimation error of the wheel angular velocity and based on a LuGre model can be used for this purpose (Patel, 2006).

We now consider an adhesion-torque observer for estimation. In (3), we neglect the unknown disturbance torque of the wheel T_d because the dominant disturbance torque caused by the vibration of the brake caliper acts only for a moment in the initial braking time. Then the adhesion torque T_a is expressed as

$$T_a = J\dot{\omega} + B\omega + T_b \tag{25}$$

Taking Laplace transforms yields

$$T_a(s) = Js\omega(s) + B\omega(s) + T_b(s) \tag{26}$$

Since a differential term is included in (26), we implement a first-order lowpass filter of the form

$$\hat{T}_a(s) = \frac{Js}{\tau s + 1}\omega(s) + B\omega(s) + T_b(s) \tag{27}$$

or

$$\hat{T}_a(s) = \left(B + \frac{J}{\tau} - \frac{J/\tau}{\tau s + 1} \right)\omega(s) + T_b(s) \tag{28}$$

where τ is the time constant of the lowpass filter in the adhesion-torque observer, which is illustrated in Fig. 11. The estimated adhesion coefficient $\hat{\mu}$ can now be obtained by

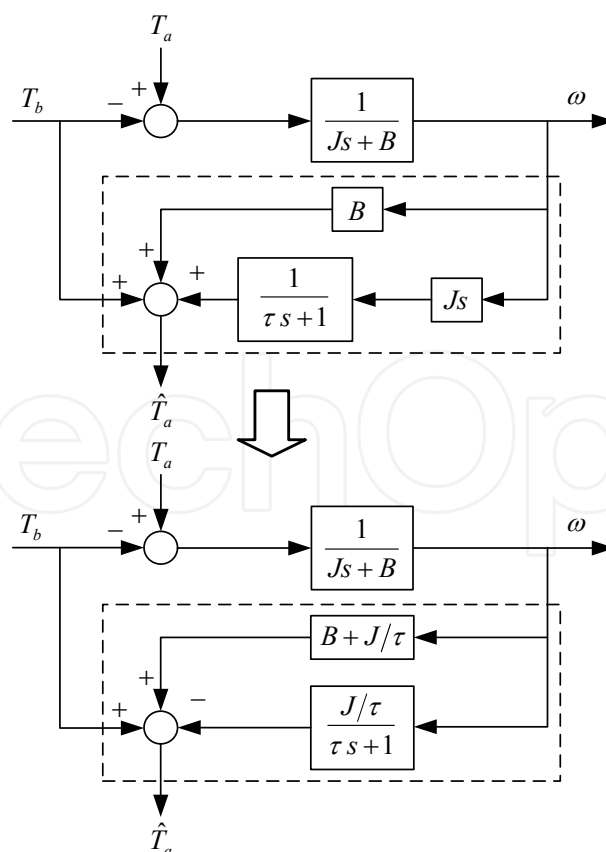$$\hat{\mu} = \frac{\hat{T}_a}{Nr} \tag{29}$$

Fig. 11. Adhesion-torque observer.

As shown by the experimental wheel-slip results in Fig. 12, before 4.5 s, the velocity v of the rolling stocks matches the tangential velocity $v_w = r\omega$ of the wheel, where r and ω are the radius and angular velocity of the wheel, respectively, while a large difference occurs between the velocity of the rolling stocks and the tangential velocity of the wheel at 4.5 s when a large brake torque is applied. This difference means that large wheel slip occurs as a result of braking. The controller ceases the braking action at 6.1 s when the slip ratio exceeds 50%. Henceforth, the tangential velocity of the wheel recovers, and the slip ratio decreases to zero by the adhesion force between the rail and the wheel. In the experiment, to prevent damage due to excessive wheel slip, the applied brake torque is limited so that the slip ratio does not exceed 50%.
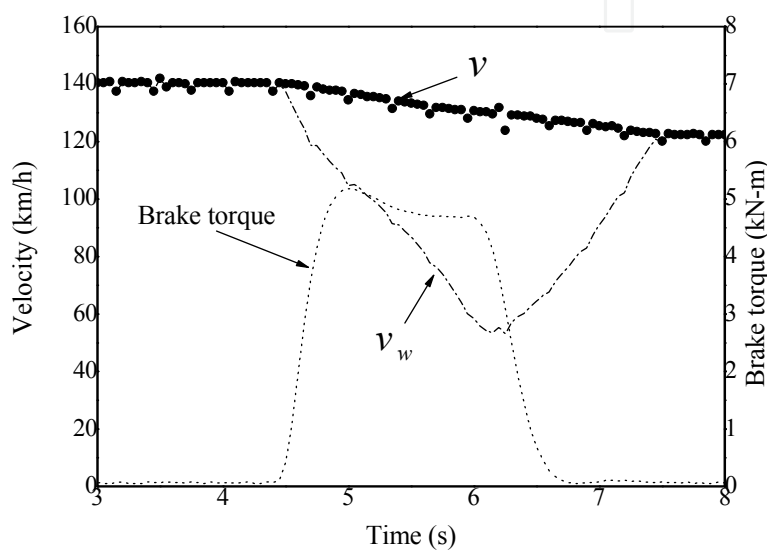

Fig. 12. Experimental wheel-slip results.

Table 2 shows the parameters of the adhesion force models for computer simulation. In Table 2, the parameter values for the length l and the width w of the contact footprint are taken from (Uchida, 2001). The constant a in (7) for the beam model is determined as 0.0013 h/km based on the adhesion experimental results at the initial braking velocity of 140 km/h.

Parameter	Notation	Value
Modulus of transverse elasticity	C_x	$1.52 \times 10^9\,\text{N/m}^2$
Length	l	0.019 m
Width	w	0.019 m
Wheel load	N	34.5 kN
Maximum adhesion coefficient for v_0 = 30, 60, 100, 140 km/h	$\mu_{\max}$	0.360, 0.310, 0.261, 0.226
Radius of the wheel	r	0.43 m

Table 2. Parameters of the beam and bristle models for computer simulation.
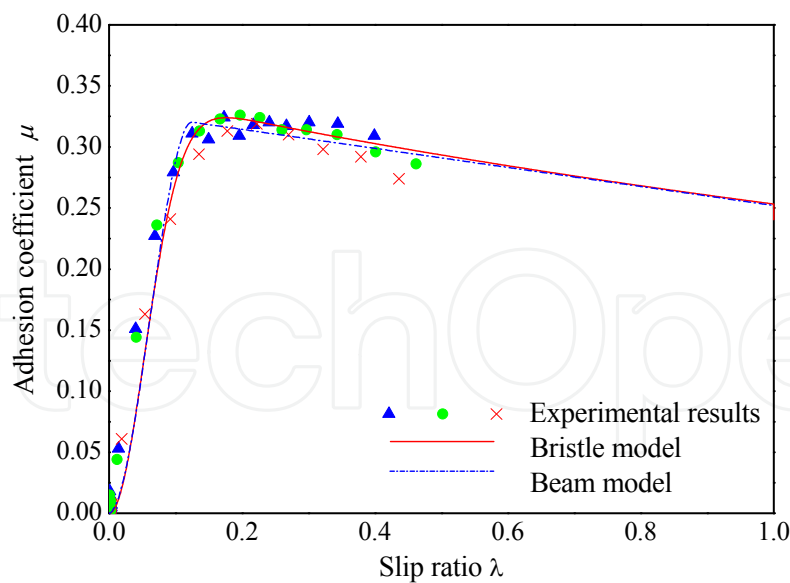
Figure 13 shows experimental and simulation results of the adhesion coefficient according to the slip ratio and initial braking velocity. As shown in Fig. 13, the variation of the adhesion coefficients obtained by the experiments is large. It is therefore difficult to determine a precise mathematical model for the adhesion force. In spite of these large variations, it is found that the experimental results of the mean value of the adhesion coefficient according to the slip ratio are consistent with the simulation results based on the two kinds of adhesion force models. Table 3 shows the mean values of the absolute errors between the experimental results for the mean value of the adhesion coefficient and the simulation results for the beam and bristle models according to the initial braking velocity of the rolling stocks. Mean values of the absolute errors in the relevant range of the initial braking velocity for the beam and bristle models are 0.011 and 0.0083, respectively. Using the bristle model in place of the beam model yields 24.5% improvement in accuracy.
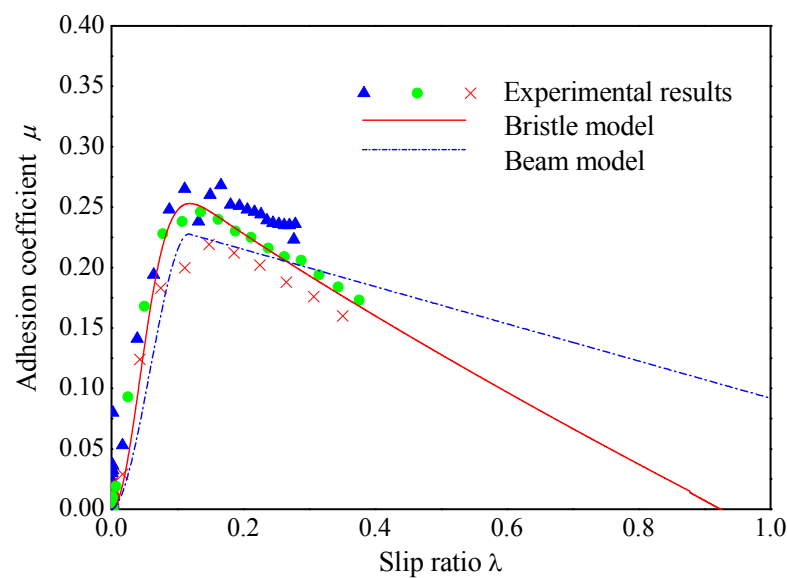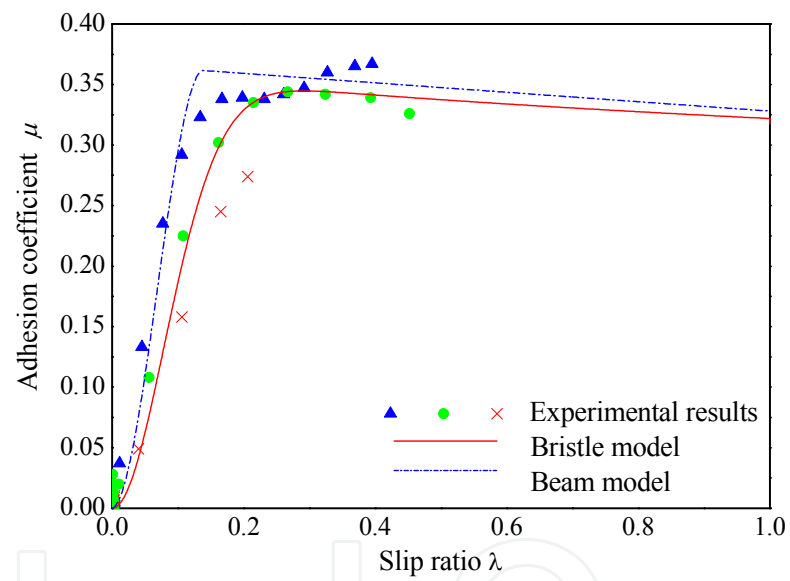

(a) Initial braking velocity v_0 = 140 km/h
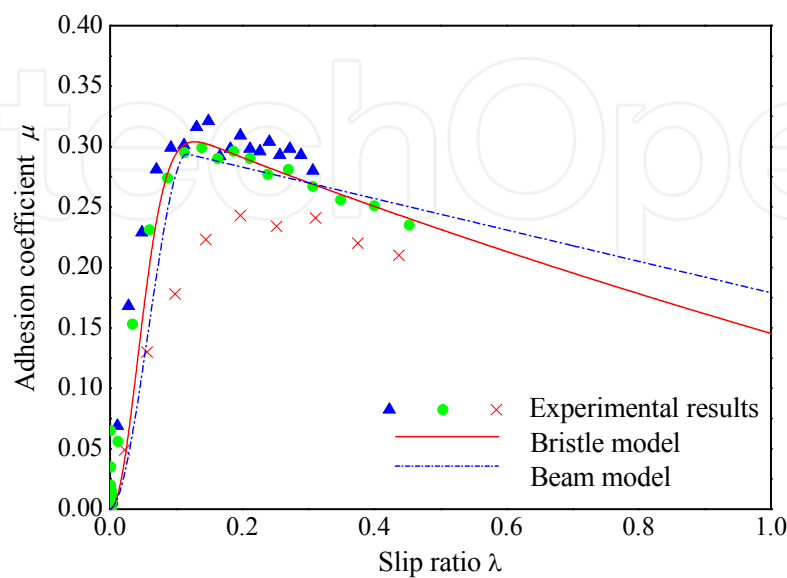
(b) Initial braking velocity v_0 = 100 km/h

(c) Initial braking velocity v_0 = 60 km/h

(d) Initial braking velocity v_0 = 30 km/h

Fig. 13. Experimental and simulation results of the adhesion coefficient.

Initial braking velocity Adhesion model	30 km/h	60 km/h	100 km/h	140 km/h
Beam model	0.0130	0.0085	0.0132	0.0093
Bristle model	0.0080	0.0080	0.0102	0.0077

Table 3. Mean values of the absolute errors between the experimental results for the mean value of the adhesion coefficient and the simulation results for the beam and bristle models.

From the experimental results in Fig. 13, the parameters α, β, and γ of the bristle model (19) - (22), (24) can be expressed as

$$\alpha = 5.455 \times 10^4 - 3.641 \times 10^2 v_0 + 3.798 \times 10^{-1} v_0^2 \tag{30}$$

$$\beta = 1.873 \times 10^{-2} - 6.059 \times 10^{-5} v_0 + 5.500 \times 10^{-8} v_0^2 \tag{31}$$

$$\gamma = 2.345 \times 10^2 - 8.620 \times 10^{-1} v_0 + 1.053 \times 10^{-4} v_0^2 \tag{32}$$

where v_0 is the initial braking velocity of the rolling stocks. The coefficients in (30), (31), and (32) are obtained by curve fitting for the values of the parameters according to the initial braking velocity.
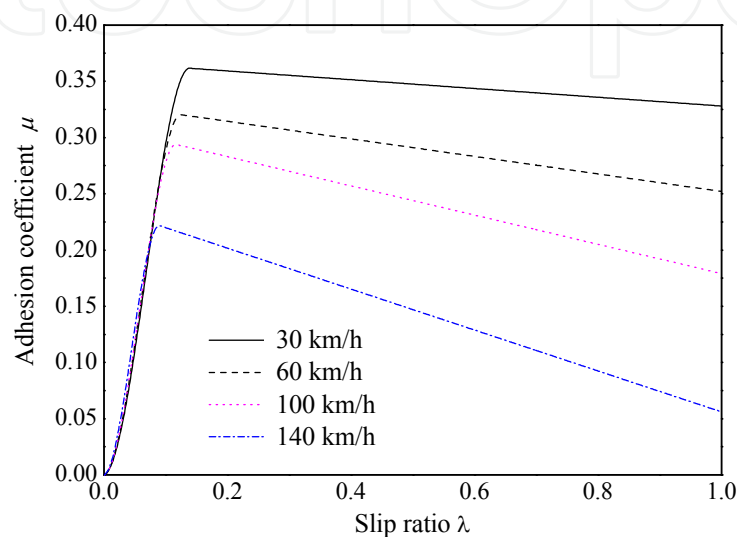

Fig. 14. Simulation results of the mean value of the adhesion coefficient for the beam model.
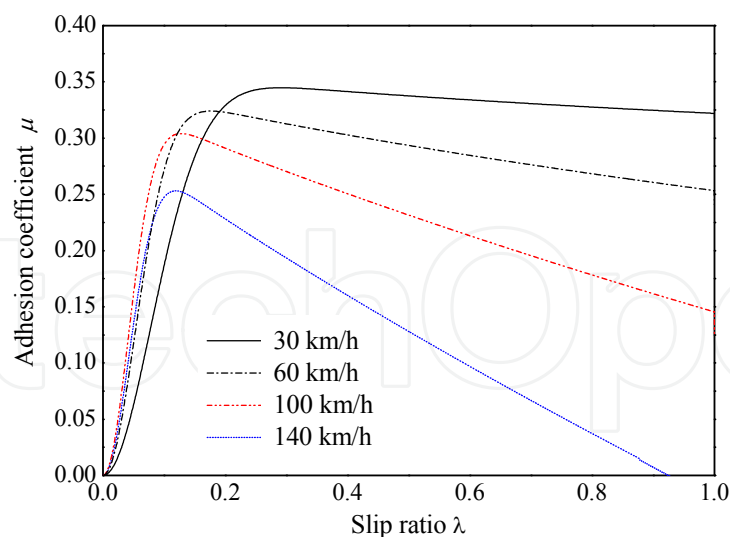

Fig. 15. Simulation results of the mean value of the adhesion coefficient for the bristle model.

Simulation results of the mean value of the adhesion coefficients for the beam model and bristle model according to the slip ratio and initial braking velocity, respectively, are shown in Fig. 14 and 15. These results show a similar tendency for the change in the initial braking velocity conditions. However, the adhesion force model based on the beam model cannot represent the dynamic characteristics of friction. The beam model is obtained by curve

fitting the experimental results on the adhesion force, while the bristle model, which includes the friction dynamics, describes the effect of the initial braking velocity accurately in the adhesion regime, where the adhesion force increases according to the slip ratio, as shown in Fig. 15. Therefore, the bristle model is more applicable than the beam model for the desired wheel-slip controller design.

6. Desired wheel slip using adaptive sliding mode control

The desired wheel-slip brake control system is designed by using an adaptive sliding mode control (ASMC) scheme to achieve robust wheel-slip brake control. In the controller design process, the random value of adhesion torque, the disturbance torque due to the vibration of the brake caliper, and the traveling resistance force of the rolling stocks are considered as system uncertainties. The mass of the rolling stocks and the viscous friction torque coefficient are also considered as parameters with unknown variations. The adaptive law for the unknown parameters is based on Lyapunov stability theory.

The sliding surface s for the design of the adaptive sliding mode wheel-slip brake control system is defined as

$$s = e + \rho \int_0^t e\,dt \tag{33}$$

where $e = \sigma_d - \sigma$ is the tracking error of the relative velocity, $\sigma = \lambda v = v - r\omega$ is the relative velocity, σ_d is the reference relative velocity, and ρ is a positive design parameter.

The sliding mode control law consists of equivalent and robust control terms, that is,

$$T_b = U_{eq} + U_r \tag{34}$$

where U_{eq} and U_r are the equivalent and robust control terms. To obtain U_{eq} and U_r, we combine (3), (4), with the derivative of the sliding surface in (33), and include random terms in the adhesion force $F_{ar} = F_a + F_r$ and the adhesion torque $T_{ar} = T_a + T_r$, where F_r and T_r are the random terms of the adhesion force and adhesion torque, respectively. Then, the derivative of the sliding surface can be written as

$$\dot{s} = \dot{\sigma}_d + \left(\frac{1}{rM} + \frac{r}{J}\right)T_a + \left(\frac{1}{rM} + \frac{r}{J}\right)T_r + \frac{1}{M}F_r - \frac{r}{J}T_b - \frac{rB}{J}\omega - \frac{r}{J}T_d + \rho e \tag{35}$$

To determine the equivalent control term U_{eq}, uncertainties such as random terms in the adhesion force and adhesion torque F_r and T_r, as well as the disturbance torque T_d in (35) are neglected, and it is assumed that the sliding surface s is at steady state, that is, $\dot{s} = 0$, then the equivalent control law can be determined as

$$U_{eq} = \frac{J}{r}\left[\dot{\sigma}_d + \left(\frac{1}{rM} + \frac{r}{J}\right)T_a - \frac{rB}{J}\omega + \rho e\right] \tag{36}$$

Thus, $\dot{s}$ can be rewritten as

$$\dot{s} = \left(\frac{1}{rM} + \frac{r}{J}\right)T_r + \frac{1}{M}F_r - \frac{r}{J}T_d - \frac{r}{J}U_r \tag{37}$$

In the standard sliding mode control, to satisfy the reachability condition that directs system trajectories toward a sliding surface where they remain, the derivative of the sliding surface is selected as

$$\dot{s} = -K \operatorname{sgn}(s) \tag{38}$$

In this case, chattering occurs in the control input. To attenuate chattering in the control input, the derivative of the sliding surface is selected as (Gao, 1993)

$$\dot{s} = -Ds - K \operatorname{sgn}(s) \tag{39}$$

where the parameters D and K are positive.

To determine a control term U_r that achieves robustness to uncertainties such as random terms in the adhesion force and adhesion torque, as well as the disturbance torque, it is assumed that

$$D_0 |s| + K_0 > \left| \left(\frac{1}{rM} + \frac{r}{J} \right) T_r + \frac{1}{M} F_r - \frac{r}{J} T_d \right| + \eta \tag{40}$$

where the parameters $D_0 = \frac{r}{J} D$, $K_0 = \frac{r}{J} K$, and η are positive. Then, the robust control law can be determined as

$$U_r = Ds + K \operatorname{sgn}(s) \tag{41}$$

and using (40), the reachability condition is satisfied as

$$
\begin{aligned}
s\dot{s} &= s \left[\left(\frac{1}{rM} + \frac{r}{J} \right) T_r + \frac{1}{M} F_r - \frac{r}{J} T_d - D_0 s - K_0 \operatorname{sgn}(s) \right] \\
&\leq |s| \left[\left| \left(\frac{1}{rM} + \frac{r}{J} \right) T_r + \frac{1}{M} F_r - \frac{r}{J} T_d \right| - D_0 |s| - K_0 \right] \\
&< -\eta |s|.
\end{aligned} \tag{42}
$$

Finally, the sliding mode control law is selected as

$$
\begin{aligned}
T_b &= U_{eq} + U_r \\
&= \frac{J}{r} \left[\dot{\sigma}_d + \left(\frac{1}{rM} + \frac{r}{J} \right) T_a - \frac{rB}{J} \omega + \rho e \right] + Ds + K \operatorname{sgn}(s),
\end{aligned} \tag{43}
$$

where the reference slip acceleration $\dot{\sigma}_d$ and the adhesion torque T_a cannot be measured during operation. Therefore, to implement the control system, the reference slip acceleration $\dot{\sigma}_d = \lambda_d \dot{v}$ must be estimated by $\lambda_d \hat{\dot{v}}$, where $\hat{\dot{v}}$ is the estimated acceleration of the rolling stocks, which can be obtained by the measured velocity of the rolling stocks through the first-order filter $G_f(s) = \frac{s}{\tau s + 1}$. In addition, the adhesion torque $T_a = r F_a$ must be replaced by the calculated value given by (20) and (22) with the measured relative velocity σ.

If the mass of the rolling stocks M and the viscous friction torque coefficient B are considered as parameters with variation, that is, $M = M_n + M_p$ and $B = B_n + B_p$, where the

subscripts n and p denote the nominal and perturbation values, respectively, then the uncertainty ψ in the mass of the rolling stocks and the viscous friction torque coefficient is defined as

$$\psi = \frac{1}{rM_p}T_m - \frac{rB_p}{J}\omega = \theta^T\phi \tag{44}$$

where $\theta^T = \begin{bmatrix} \dfrac{1}{rM_p} & -\dfrac{rB_p}{J} \end{bmatrix}$ and $\phi = \begin{bmatrix} T_m \\ \omega \end{bmatrix}$. The parameter vector θ is considered as an

unknown parameter vector, which can be estimated by using the update law. From (43) and the estimated unknown parameter vector $\hat{\theta}$, the estimated sliding model control law can be selected as

$$\hat{T}_b = \frac{J}{r}\left[\dot{\sigma}_d + \left(\frac{1}{rM_n} + \frac{r}{J}\right)T_m - \frac{rB_n}{J}\omega + \hat{\theta}^T\phi + \rho e\right] + Ds + K\,\mathrm{sgn}(s) \tag{45}$$

In order to obtain the update law for the unknown parameters, we consider the Lyapunov candidate

$$V = \frac{1}{2}s^2 + \frac{1}{2k}\tilde{\theta}^T\tilde{\theta} \tag{46}$$

where $\tilde{\theta} = \theta - \hat{\theta}$, θ and $\hat{\theta}$ are the nominal and estimated parameter vectors, respectively, and k is a positive parameter. The derivative of the Lyapunov candidate including sliding dynamics is expressed as

$$\dot{V} = s\left[\dot{\sigma}_d + \left(\frac{1}{rM_n} + \frac{r}{J}\right)T_m - \frac{rB_n}{J}\omega - \frac{r}{J}\hat{T}_b + \theta^T\phi + \rho e\right] - \frac{1}{k}\tilde{\theta}^T\dot{\hat{\theta}} \tag{47}$$

Substituting the estimated brake torque $\hat{T}_b$ given by (45) into (47) yields

$$\dot{V} = -Ds^2 - Ks\,\mathrm{sgn}(s) + \tilde{\theta}^T\left(s\phi - \frac{1}{k}\dot{\hat{\theta}}\right) \tag{48}$$

By using the update law for the unknown parameters given by

$$\dot{\hat{\theta}} = ks\phi \tag{49}$$

the derivative of the Lyapunov candidate (48) is nonpositive. The invariant set theorem then guarantees asymptotic stability of the wheel-slip brake control system (Khalil, 1996).

7. Performance evaluation of the desired wheel-slip control system

The characteristics of the wheel-slip control system shown in Fig. 16 are evaluated by simulation. The performance and robustness of the wheel-slip control system using the ASMC scheme are evaluated for railway rolling stocks, while considering system uncertainties such as parameter variation, railway conditions, disturbances, and unmodeled dynamics.

For simulation, the bristle model is used for the adhesion force model because the bristle model is relatively close to the actual adhesion force compared with the beam model. In addition, it is assumed that the brake torque is applied when the velocity of the rolling stocks is 100 km/h. From the experimental results in Fig. 13, it is assumed that the random adhesion force F_r is a white noise signal with a Gaussian distribution that has a standard deviation of 0.431 kN. Since the actual brake force is applied to the wheel disk by the brake caliper, the vibration occurs on the brake caliper at the initial braking moment. Therefore, the disturbance torque $T_d = 0.05 T_b e^{-4t} \sin 10\pi t$, caused by the vibration of the brake caliper, is considered in the simulation. In addition, the traveling resistance force $F_r = 0.63 v^2$ of the rolling stocks and the viscous friction $B = 0.25^{-0.01t}$ is considered, which causes overheating between the wheel disk and the brake pad. Finally, the unmodeled dynamics $G_a(s) = \dfrac{e^{-0.15s}}{0.6s + 1}$ of the pneumatic actuator of the brake control system are considered.
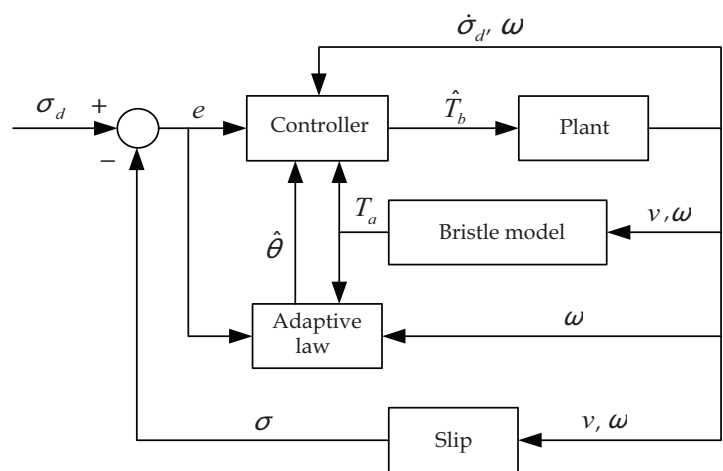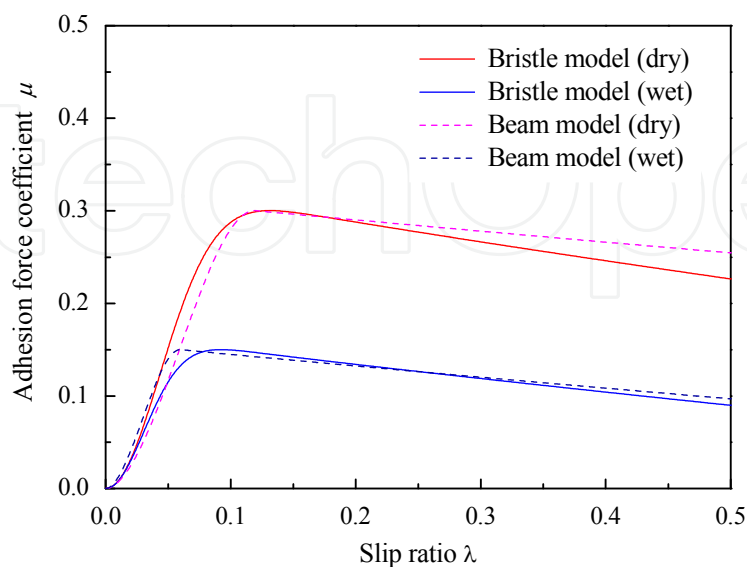

Fig. 16. Wheel-slip control system.

Fig. 17. Relationship between the adhesion force coefficient and the slip ratio according to the change in rail conditions from dry to wet based on the beam and bristle models.

To assess the braking performance in the presence of parameter variations, the simulation is carried out under the assumption that the mass of the rolling stocks changes according to the number of passengers and that the rolling stocks travel in dry or wet rail conditions. It is assumed that the mass of the rolling stocks changes from 3517 to 5276 kg at 25 s. It is also assumed that the maximum adhesion force under wet rail conditions is approximately half of the maximum adhesion force under dry rail conditions and that the rail conditions change from dry to wet at 25 s. Figure 17 shows the relationship between the adhesion force coefficient and the slip ratio according to the change in rail conditions from dry to wet based on the beam and bristle models, which are considered in the simulation. As shown in Fig. 17, the reference slip ratio is assumed to be 0.119 and 0.059 under dry and wet rail conditions, respectively, for the beam model, and 0.132 and 0.092 under dry and wet rail conditions, respectively, for the bristle model.

In order to verify the performance and robustness of the ASMC system, the desired wheel-slip control system using the ASMC scheme is compared with a PI control system through simulation. Control gains of the PI and ASMC systems are selected by trial and error by considering various constraints for each case, such as the maximum brake torque and the maximum slip ratio allowed until the desired performance and robustness are obtained, which are summarized in Table 4. In controller design, the bristle model and beam model are considered for the adhesion force model.

Control scheme	Control gain	Beam model	Bristle model
PI	K_p	400 N-h	650 N-h
	K_i	54 N	27 N
ASMC	D	1.62 h^{-1}	1.53 h^{-1}
	K	70 km/h^2	70 km/h^2
	ρ	1.65 h^{-1}	1.54 h^{-1}
	k	2.1×10^{-8}	2.1×10^{-8}

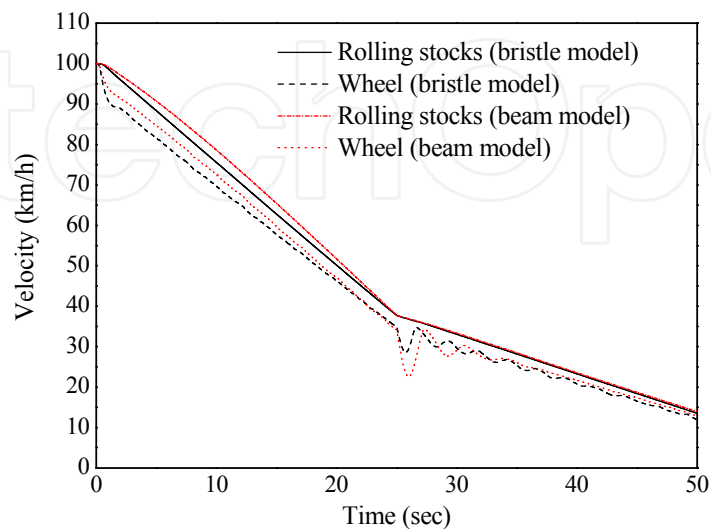Table 4. Control gains of the PI and ASMC systems.

Fig. 18. Velocities of the wheel and rolling stocks for the PI control systems based on the beam and bristle models.
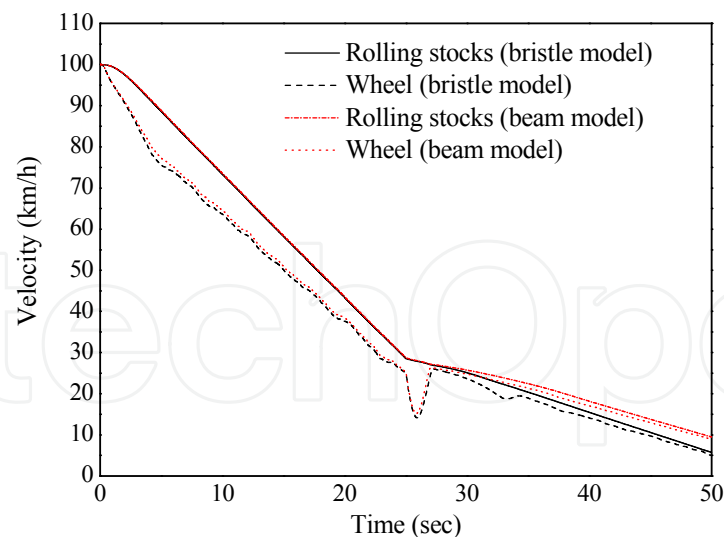
Fig. 19. Velocities of the wheel and rolling stocks for the adaptive sliding mode control (ASMC) systems based on the beam and bristle models.

Figures 18 and 19 show the velocities of the wheel and rolling stocks for the PI and ASMC systems based on the beam and bristle models, respectively. As shown in Fig. 18, the braking distance and time of the PI control system until the velocity of the rolling stocks reaches 5 km/h are 700 m and 59.5 s, respectively, for the PI control based on the beam model, and 682 m and 58.9 s, respectively, for the PI control based on the bristle model. By using the PI control based on the bristle model in place of the PI control based on the beam model, the braking distance and time are improved by 2.6% and 1%, respectively. However, the PI control system cannot effectively compensate for system uncertainties such as the mass of the rolling stocks, railway conditions, the traveling resistance force, and variations of the viscous friction coefficient.

As shown in Fig. 19 for the ASMC system, the braking distance and time are 607 m and 55.3 s, respectively, for the ASMC based on the beam model and 581 m and 50.7 s, respectively, for the ASMC based on the bristle model. Figure 19 shows that the ASMC system provides robust velocity regulation of the rolling stocks in the presence of variations in the mass of the rolling stocks and rail conditions. In this case, the braking distance and time are improved by 4.3% and 8.3%, respectively, by using the ASMC based on the bristle model in place of the ASMC based on the beam model.

Figure 20 shows the brake torques for the PI and ASMC systems based on the beam and bristle models. The expended braking energies of the PI and ASMC systems during braking time are 1.77×10^7 N-m and 1.71×10^7 N-m, respectively. Therefore, by using the adaptive sliding mode control system, it is possible to effectively reduce the braking time and distance using a relatively small braking energy consumption.

The operation of the PI and ASMC wheel-slip control systems can also be demonstrated through the slip ratios. Figure 21 shows the slip ratios of the PI and ASMC systems based on the beam and bristle models. Figure 21 shows that the PI control system has a large tracking error of slip ratio compared with the ASMC system. However, the wheel-slip control system using the ASMC scheme can maintain the slip ratio near the reference slip ratio during the braking time although the slip ratios fluctuate slightly after 25s when the system uncertainties are applied. Therefore, it is appropriate to use the adaptive sliding mode control system to obtain the maximum adhesion force and a short braking distance. Using the ASMC based on the bristle model in place of the PI control based on the beam model

yields 28% improvement in the wheel slip. Table 5 summarizes the performance of the PI and ASMC systems based on the beam and bristle models.
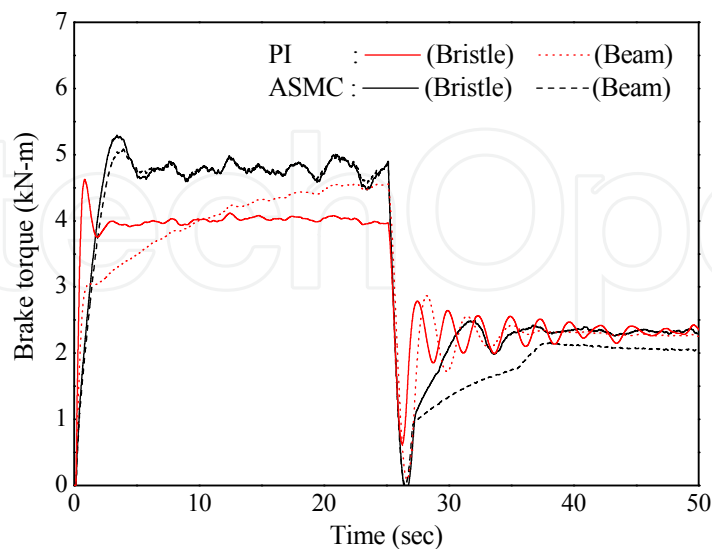

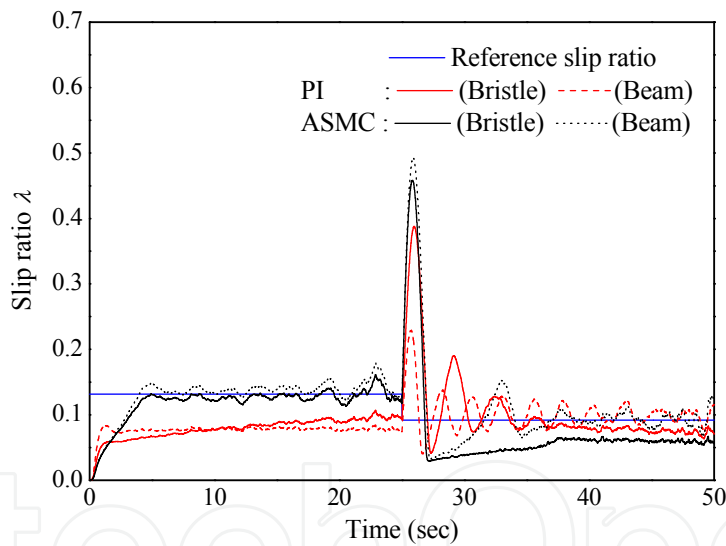Fig. 20. Brake torques for the PI and ASMC systems based on the beam and bristle models.

Fig. 21. Slip ratios of the PI and ASMC systems based on the beam and bristle models.

Performance	PI		ASMC	
	Beam model	Bristle Model	Beam model	Bristle model
Braking distance (m)	700	682	607	581
Braking time (s)	59.5	58.9	55.3	50.7
Expended braking energy(kN-m)	1.77×10^7	1.77×10^7	1.77×10^7	1.77×10^7
Mean value of the absolute error between λ and λ_d	0.0378	0.0351	0.0354	0.0272

Table 5. The performances of the PI and ASMC systems based on the beam and bristle models.

8. Conclusions

Two kinds of models, namely, the beam and bristle models, for the adhesion force in railway rolling stocks are developed. The validity of the beam and bristle models is obtained through an adhesion test using a brake performance test rig. By comparing the simulation results of the two kinds of adhesion force models with the experimental results, it is found that the two kinds of adhesion force models can effectively represent the experimental results. However, the adhesion force model based on the beam model cannot represent the dynamic characteristics of friction, while the bristle model can mathematically include the dynamics on friction and can precisely consider the effect of the initial braking velocity in the adhesion regime. Therefore, the bristle model is more appropriate than the beam model for the design of the wheel-slip controller.

In addition, based on the beam and bristle models, the PI and ASMC systems are designed to control wheel slip in railway rolling stocks. Through simulation, we evaluate the performance and robustness of the PI and ASMC systems based on the beam and bristle models for railway rolling stocks. It is verified from the simulation study that, among the four types investigated according to control schemes and adhesion force models, the adaptive sliding mode control system based on the bristle model is the most suitable system for the wheel slip in the rolling stocks with system uncertainties such as the mass and traveling resistance force of the rolling stocks, rail conditions, random adhesion torque, disturbance torque due to the vibration of the brake caliper, and unmodeled actuator dynamics.

9. References

L. Alvarez, J. Yi, R. Horowitz, and L. Olmos (2005), Dynamic friction model-based tire-road friction estimation and emergency braking control, *ASME Journal of Dynamic Systems, Measurement, and Control*, vol. 127, no. 1, pp. 22-32.

M. Basset, C. Zimmer, and G. L. Gissinger (1997), Fuzzy approach to the real time longitudinal velocity estimation of a FWD car in critical situations, *Vehicle System Dynamics*, vol. 27, no. 5 & 6, pp. 477-489.

C. Canudas de Wit, and P. Tsiotras (1999), Dynamic tire friction models for vehicle traction control, *Proceedings of the 38th IEEE Conference on Decision and Control,* Phoenix, Arizona, pp. 3746-3751.

C. Canudas de Wit, and P. Lischinsky (1997), Adaptive friction compensation with partially known dynamic model, *International Journal of Adaptive Control Signal Processing,* vol. 11, pp. 65-80.

C. Canudas de Wit, K. J. Astrom, and P. Lischinsky (1995), A new model for control of systems with friction, *IEEE Transaction on Automatic Control,* vol. 40, no. 3, pp. 419-425.

G. Charles, and R. Goodall (2006), Low adhesion estimation, *Proceedings of the Institution of Engineering and Technology International Conference on Railway Condition Monitoring*, Birmingham, UK, pp. 96-101.

P. Dahl (1976), Solid friction damping of mechanical vibrations, *AIAA Journal,* vol. 14, no. 12, pp. 1675-1682.

W. Gao, and J. C. Hung (1993), Variable structure control of nonlinear systems, *IEEE Transaction on Industrial Electronics,* vol. 40, no. 1, pp. 45-55.

I. P. Isaev, and A. L. Golubenko (1989), Improving experimental research into adhesion of the locomotive wheel with the rail, *Rail International,* vol. 20, no. 8, pp. 3-10.

X. S. Jin, W. H. Zhang, J. Zeng, Z. R. Zhou, Q. Y. Liu, and Z. F. Wen (2004), Adhesion experiment on a wheel/rail system and its numerical analysis, *IMechE J. of Engineering Tribology,* vol. 218, pp. 293-303.

T. A. Johansen, I. Petersen, J. Kalkkuhl, and J. Lüdemann, "Gain-scheduled wheel slip control in automotive brake systems," IEEE Transactions on Control Systems Technology, vol. 11, no. 6, pp. 799-811.

S. Kadowaki, K. Ohishi, S. Yasukawa, and T. Sano (2004), Anti-skid re-adhesion control based on disturbance observer considering air brake for electric commuter train, *The 8th* IEEE *International Workshop on Advanced Motion Control, Kawasaki, Japan*, pp. 607-612.

J. J. Kalker, and J. Piotrowski (1989), Some new results in rolling contact, *Vehicle System Dynamics,* vol. 18, no. 4, pp. 223-242.

H. K. Khalil (1996), *Nonlinear systems.* Upper Saddle River, NJ: Prentice Hall

S. Kumar, M. F. Alzoubi, and N. A. Allsayyed (1996), Wheel/rail adhesion wear investigation using a quarter scale laboratory testing facility, *Proceedings of the 1996 ASME/IEEE Joint Railroad Conference*, Oakbrook, IL, pp. 247-254.

K. J. Lee, H. M. Kim, and J. S. Kim (2004), Design of a chattering-free sliding mode controller with a friction compensator for motion control of a ball-screw system, *IMechE J. of Systems and Control Engineering,* vol. 218, pp. 369-380.

L. Li, F. Y. Wang, and Q. Zhou (2006), Integrated longitudinal and lateral tire/road friction modeling and monitoring for vehicle motion control, *IEEE Transactions on Intelligent Transportation Systems,* vol. 7, no. 1, pp. 1-19.

K. Ohishi, K. Nakano, I. Miyashita, and S. Yasukawa (1998), Anti-slip control of electric motor coach based on disturbance observer, *The 5th IEEE International Workshop on Advanced Motion Control,* Coimbra, Portugal, pp. 580-585.

N. Patel, C. Edwards, and S. K. Spurgeon (2006), A sliding mode observer for tyre friction estimation during braking, *Proceedings of the 2006 American Control Conference*, Minneapolis, Minnesota, pp. 5867-5872.

H. Sakai (1987), *Tire Engineering.* Tokyo, Japan: Grand Prix Publishing, Japanese

Y. Shimizu, K. Ohishi, T. Sano, S. Yasukawa, and T. Koseki (2007), Anti-slip/skid re-adhesion control based on disturbance observer considering bogie vibration, *Proceedings of the Fourth Power Conversion Conference*, Nagoya, Japan, pp. 1376-1381.

S. Shirai (1977), Adhesion phenomena at high-speed range and performance of an improved slip-detector, *Quarterly Report of Railway Technical Research Institute*, vol. 18, no. 4, pp. 189-190.

S. Uchida, "Brake of railway III (2001), *Japan Train Operation Association Journal, Brake of Railway Vehicles*, vol. 3, pp. 25-28.

T. Watanabe, and M. Yamashita (2001), A novel anti-slip control without speed sensor for electric railway vehicles, *The 27th Annual Conference of the IEEE Industrial Electronics Society,* Denver, CO, vol. 2, pp. 1382-1387.

J. Yi, L. Alvarez, and R. Horowitz (2002), Adaptive emergency braking control with underestimation of friction coefficient, *IEEE Transactions on Control Systems Technology*, vol. 10, no. 3, pp. 381-392.
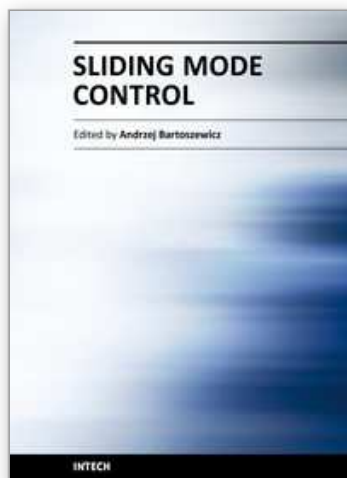
Sliding Mode Control

Edited by Prof. Andrzej Bartoszewicz

The main objective of this monograph is to present a broad range of well worked out, recent application studies as well as theoretical contributions in the field of sliding mode control system analysis and design. The contributions presented here include new theoretical developments as well as successful applications of variable structure controllers primarily in the field of power electronics, electric drives and motion steering systems. They enrich the current state of the art, and motivate and encourage new ideas and solutions in the sliding mode control area.

How to reference

In order to correctly reference this scholarly work, feel free to copy and paste the following:

Jong Shik Kim, Sung Hwan Park, Jeong Ju Choi and Hiro-o Yamazaki (2011). Adaptive Sliding Mode Control of Adhesion Force in Railway Rolling Stocks, Sliding Mode Control, Prof. Andrzej Bartoszewicz (Ed.), ISBN: 978-953-307-162-6, InTech, Available from: http://www.intechopen.com/books/sliding-mode-control/adaptive-sliding-mode-control-of-adhesion-force-in-railway-rolling-stocks

INTECH
open science | open minds